Tables and Figures

Meteorological modes of variability for fine particulate matter ($PM_{2.5}$) air quality in the United States: implications for $PM_{2.5}$ sensitivity to climate change

A. P. K. Tai, L. J. Mickey, D. J. Jacob, E. M. Leibensperger, L. Zhang, J. A. Fisher, H. O. T. Pye

Table 1. Meteorological variables used for $PM_{2.5}$ correlation analysis.[a]

Variable	Meteorological parameter
x_1	Surface air temperature (K) [b]
x_2	Surface air relative humidity (%) [b]
x_3	Surface precipitation (mm d^{-1})
x_4	Geopotential height at 850 hPa (km)
x_5	Sea level pressure tendency dSLP/dt (hPa d^{-1})
x_6	Surface wind speed (m s^{-1}) [b, c]
x_7	East-west wind direction indicator cosθ (dimensionless) [d]
x_8	North-south wind direction indicator sinθ (dimensionless) [d]

a. Assimilated meteorological data with 0.5°×0.667° horizontal resolution from the NASA Goddard Earth Observing System (GEOS-5). All data used are 24-h averages, and are deseasonalized and detrended as described in the text.

b. At 6 m above the surface (0.994 sigma level).

c. Calculated from the horizontal wind vectors (u, v).

d. θ is the angle of the horizontal wind vector counterclockwise from the east. Positive values of x_7 and x_8 indicate westerly and southerly winds, respectively.

Table 2. Dominant meteorological modes for regional $PM_{2.5}$ variability.

US Region	$PM_{2.5}$ variability explained [a]		PC regression coefficient γ_j [b]		Description [c]
	EPA-AQS	GEOS-Chem	EPA-AQS	GEOS-Chem	
Northeast	17%	21%	-0.31	-0.33	Cold front associated with mid-latitude cyclone
Midwest	29%	25%	-0.41	-0.38	
Southeast	31%	15%	-0.42	-0.29	
Pacific NW	36%	45%	-0.35	-0.39	Synoptic-scale maritime inflow
California	26%	13%	-0.28	-0.21	

a. From Eq. (5).

b. From Eq. (4).

c. For positive phases of the dominant PC.

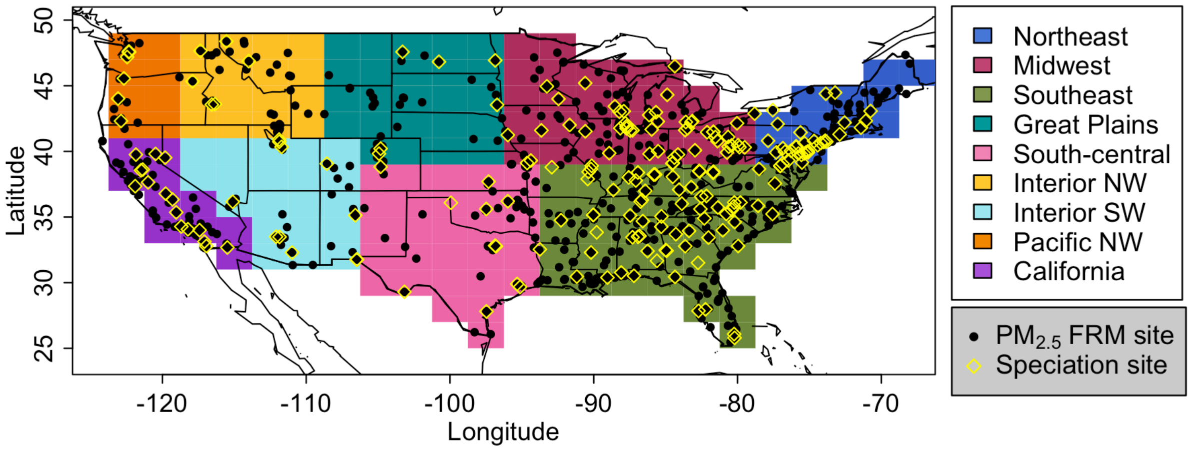

Figure 1. US regions used to study the correlations of $PM_{2.5}$ with meteorological modes of variability. Also shown are the EPA Air Quality System (AQS) $PM_{2.5}$ monitoring sites in 2006, including total $PM_{2.5}$ monitors using the Federal Reference Method (FRM) and chemical speciation monitors from the SLAMS + STN networks.

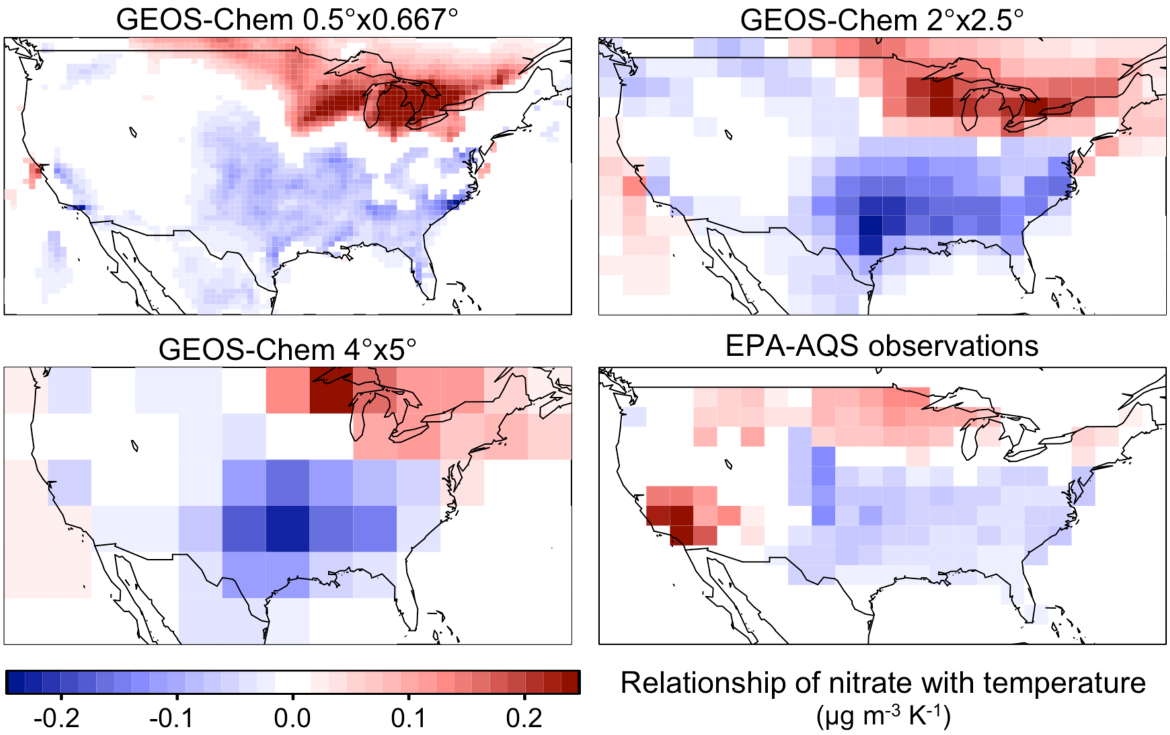

Figure 2. Simulated (2005-2007) and observed (2004-2008) relationships of nitrate $PM_{2.5}$ with surface air temperature, as measured by the multiple linear regression coefficient β_1* in Eq. (2) with units of μg m^{-3} K^{-1}. Simulated relationships are shown for three different GEOS-Chem model resolutions: 0.5°×0.667°, 2°×2.5° and 4°×5°. Observations are averaged over the 2°×2.5° grid. Values are for deseasonalized and detrended variables and are only shown when significant with 95% confidence (p-value < 0.05).

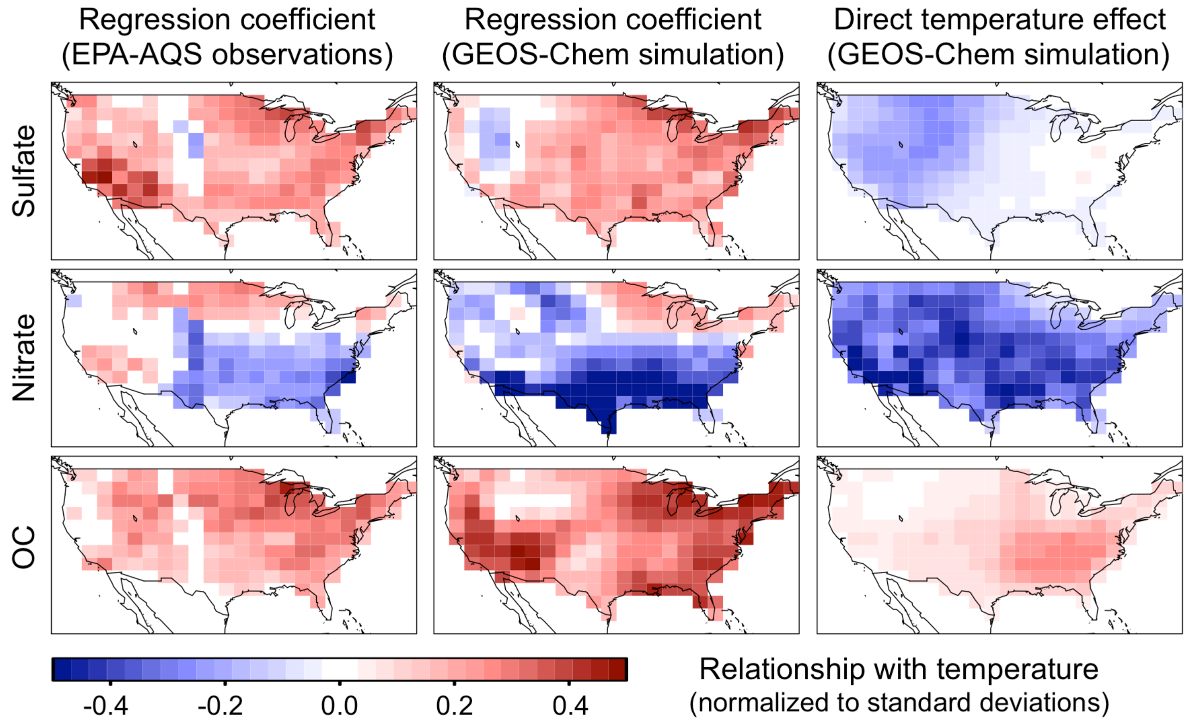

Figure 3. Relationships of sulfate, nitrate, and organic carbon (OC) $PM_{2.5}$ concentrations with surface air temperature. The left and middle panels show the observed (2004-2008) and simulated (2005-2007) standardized regression coefficients β_1 in Eq. (1). Values are for deseasonalized and detrended variables and are only shown when significant with 95% confidence (p-value < 0.05). The right panels show the direct effects of temperature on sulfate, nitrate and OC as determined by applying a global +1 K temperature perturbation in the GEOS-Chem simulation, and normalizing the results to the standard deviations of deseasonalized concentrations and temperatures to allow direct comparison to β_1.

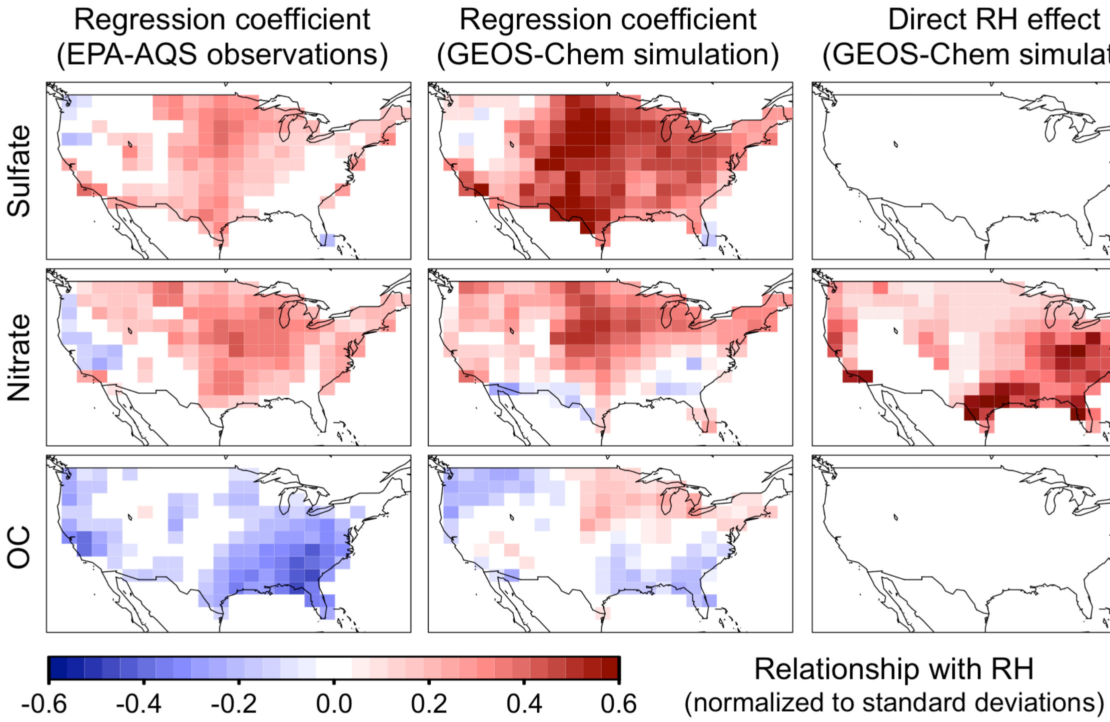

Figure 4. Same as Fig. 3 but for relative humidity (RH). The right panels show the direct effects of RH as determined by applying a global -1 % RH perturbation in the GEOS-Chem simulation.

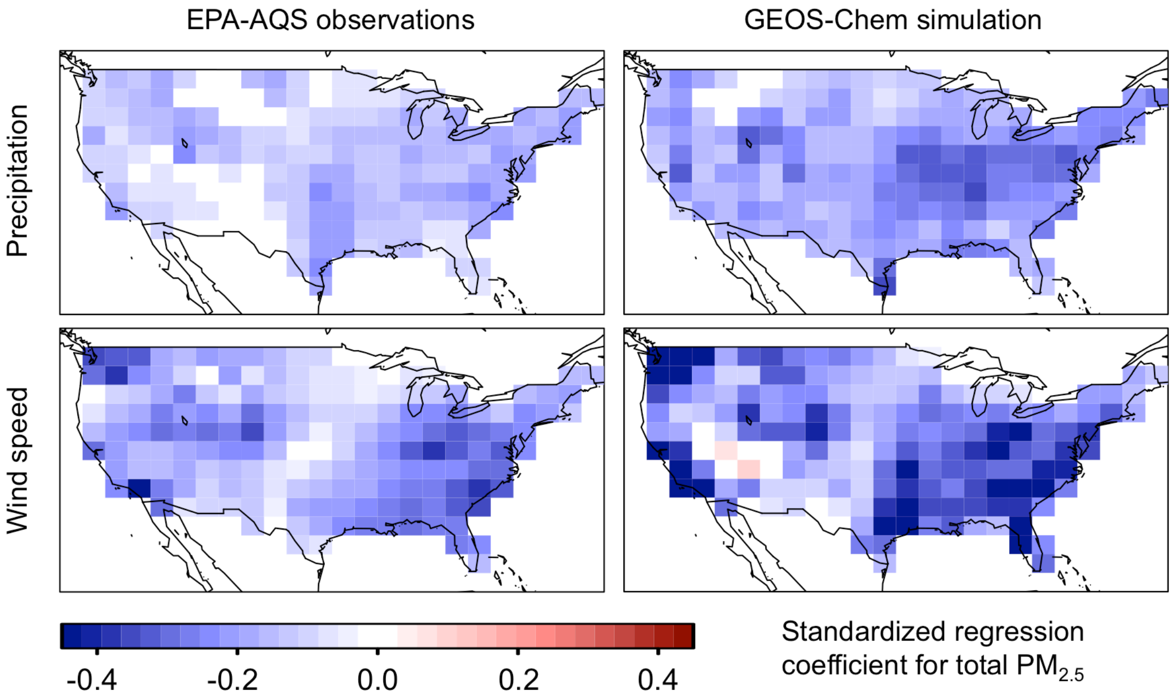

Figure 5. Relationships of total $PM_{2.5}$ concentrations with precipitation and wind speed, expressed as the standardized regression coefficients β_3 and β_6, respectively. The left panels show observations (2004-2008) and the right panels model values (2005-2007). Values are for deseasonalized and detrended variables and are only shown when significant with 95% confidence (p-value < 0.05).

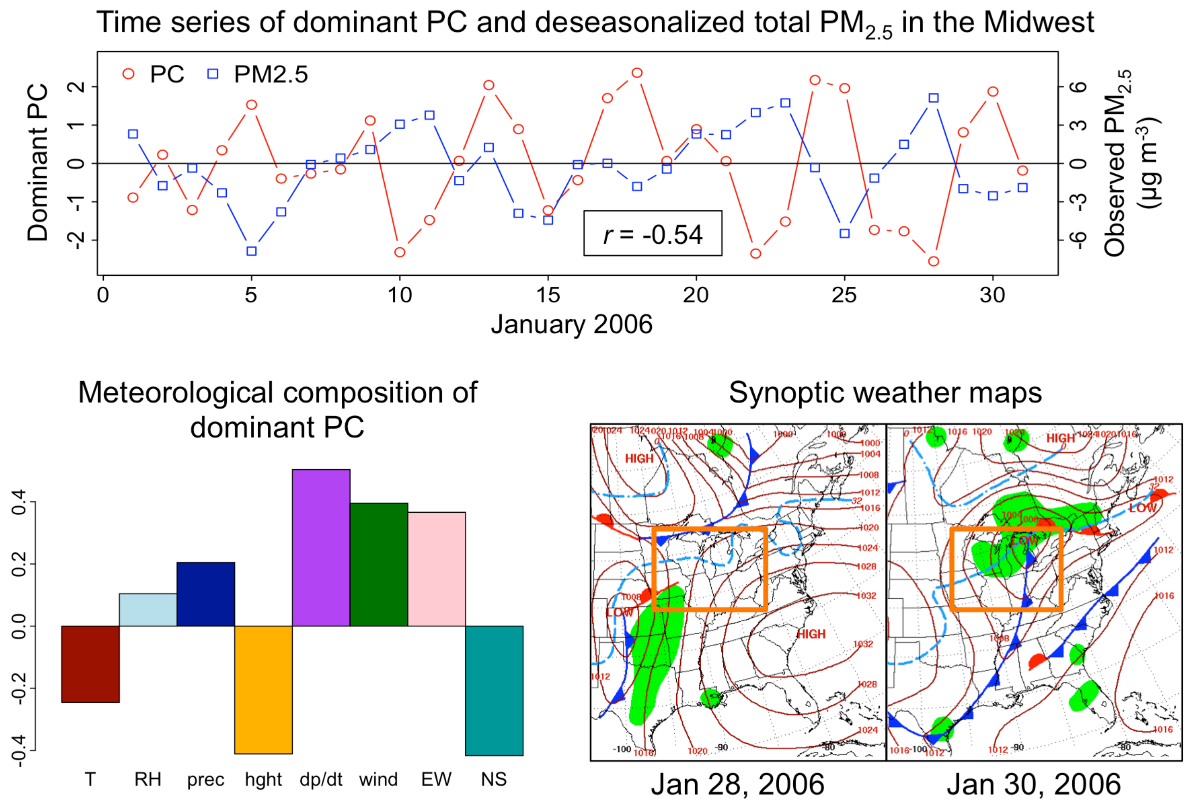

Figure 6. Dominant meteorological mode for observed $PM_{2.5}$ variability in the Midwest inferred from the principal component analysis. Top panel: time series of deseasonalized observed total $PM_{2.5}$ concentrations and the dominant meteorological mode or principal component (PC) in January 2006. Bottom left: composition of this dominant mode as measured by the coefficients α_{ki} in Eq. (3). Meteorological variables (x_k) are listed in Table 1. Bottom right: synoptic weather maps from the National Center for Environmental Prediction (NCEP) (http://www.hpc.ncep.noaa.gov/dailywxmap/) for 28 and 30 January, corresponding to maximum negative and positive influences from the principal component. The Midwest is delineated in orange.

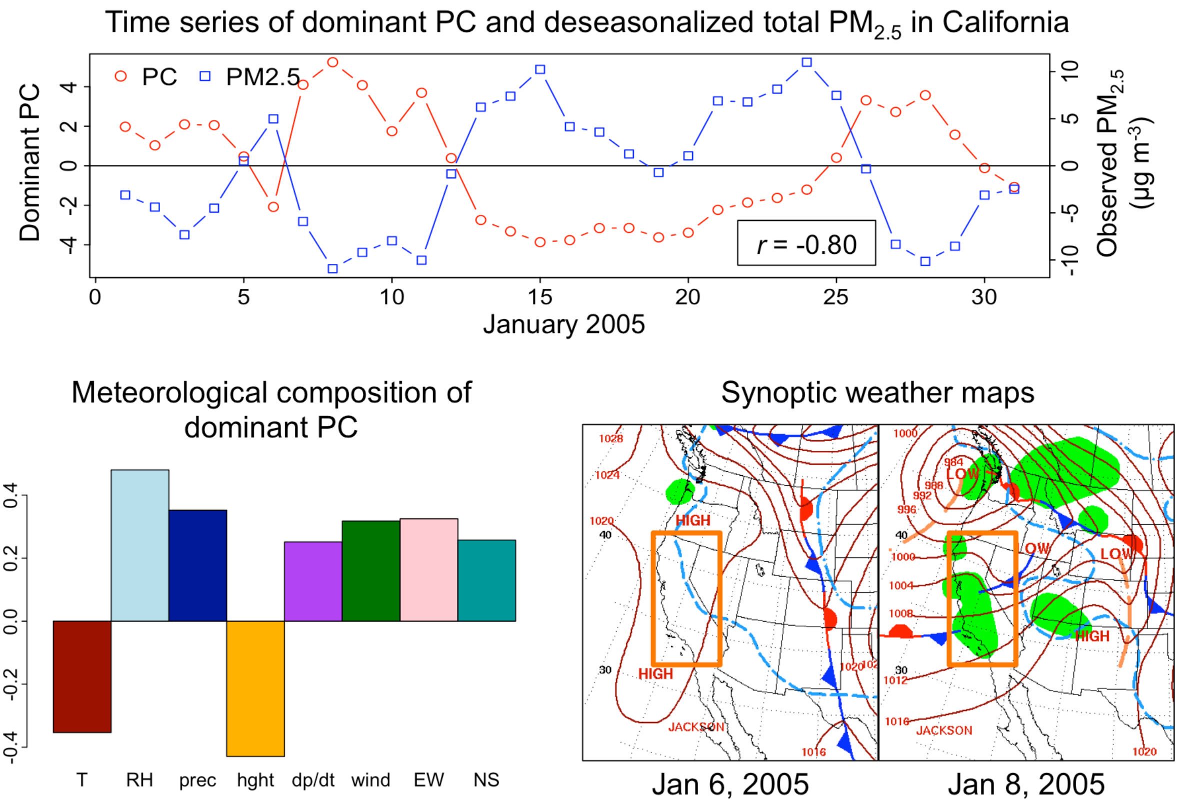

Figure 7. Same as Fig. 6 but for California.

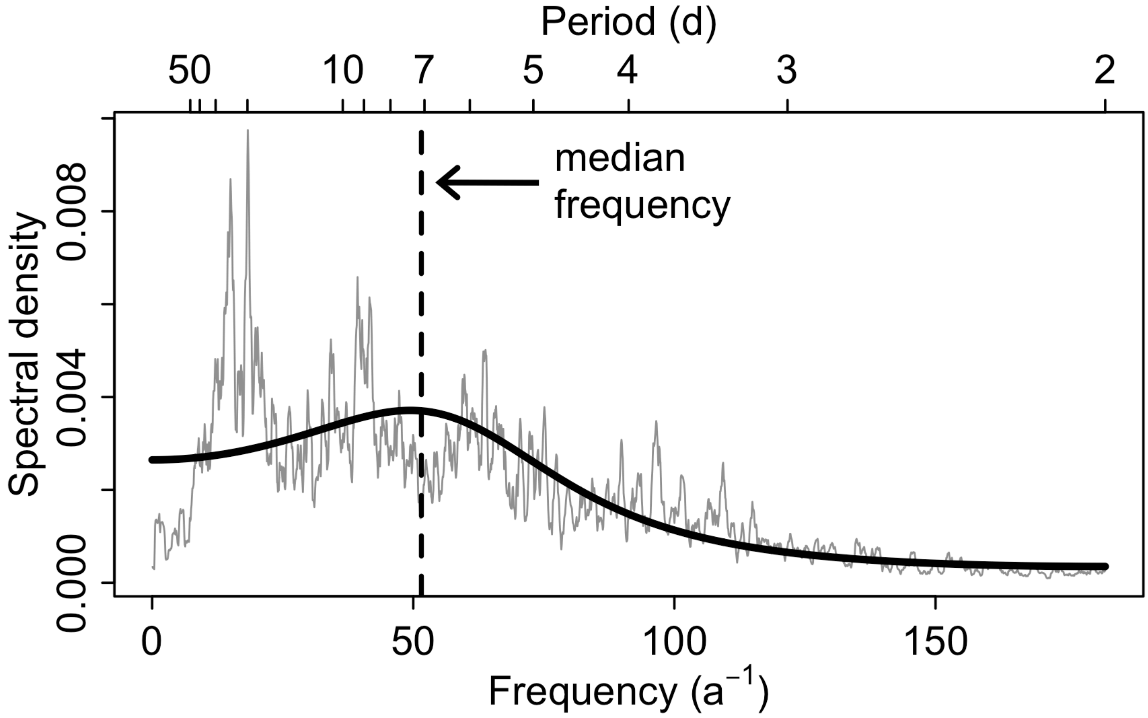

Figure 8. Frequency spectrum of the daily time series of the dominant meteorological mode (cyclone/frontal passages) in the US Midwest (Fig. 1) for 1999-2010 using NCEP/NCAR Reanalysis 1 data. The thin line shows the fast Fourier transform (FFT) spectrum and the thick line shows the smoothed spectrum from a second-order autoregressive (AR2) model. The vertical dashed line indicates the median AR2 spectral frequency used as a metric of cyclone frequency.

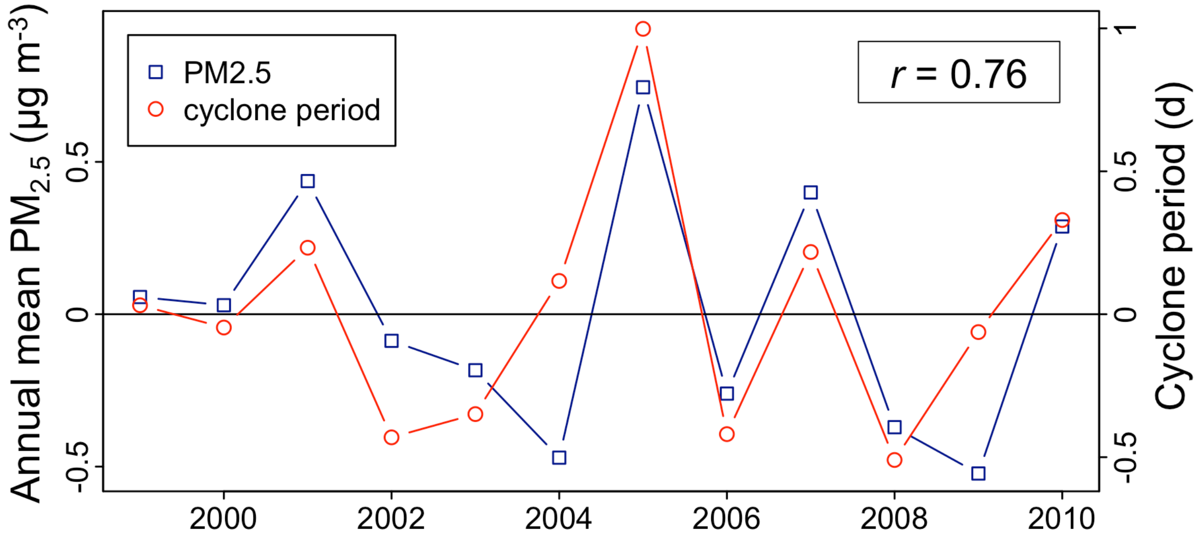

Figure 9. Anomalies of annual mean $PM_{2.5}$ concentrations and median cyclone periods for the US Midwest (Fig. 1).

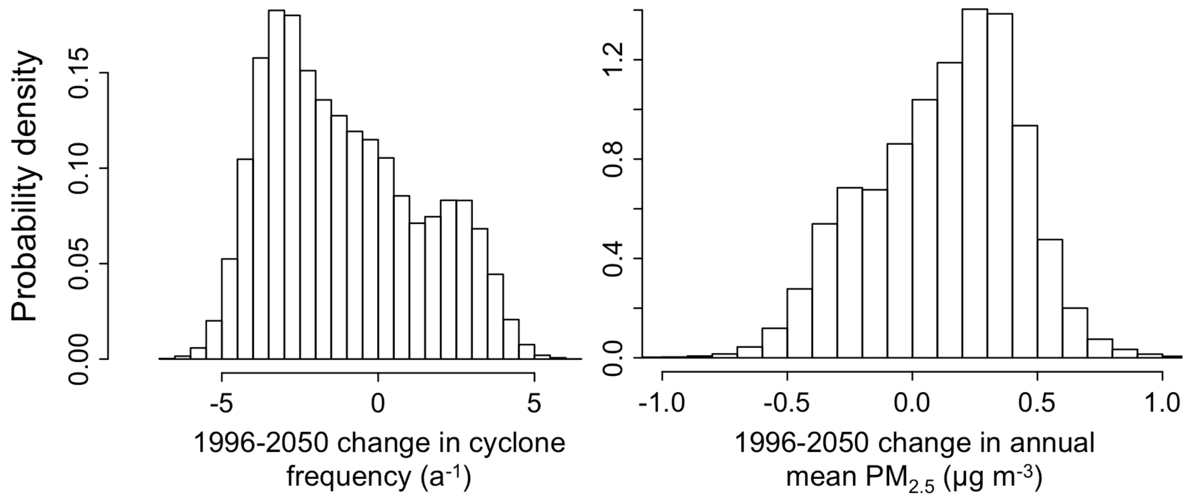

Figure 10. Probability distribution for the change in median cyclone frequency in the US Midwest between 1996-2010 and 2036-2050, and the corresponding change in annual mean $PM_{2.5}$ concentrations. Results are from five realizations of the NASA Goddard Institute for Space Studies (GISS) GCM III applied to the IPCC A1B scenario of greenhouse gas and aerosol forcings.